Optimization of constrained density functional theory

David D. O'Regan[1,*] and Gilberto Teobaldi[2,3,†]

[1] *School of Physics, CRANN and AMBER, Trinity College Dublin, Dublin 2, Ireland*
[2] *Stephenson Institute for Renewable Energy and Department of Chemistry, The University of Liverpool, L69 3BX Liverpool, United Kingdom*
[3] *Beijing Computational Science Research Center, Beijing 100094, China*

(Dated: June 16, 2016)

Constrained density functional theory (cDFT) is a versatile electronic structure method that enables ground-state calculations to be performed subject to physical constraints. It thereby broadens their applicability and utility. Automated Lagrange multiplier optimisation is necessary for multiple constraints to be applied efficiently in cDFT, for it to be used in tandem with geometry optimization, or with molecular dynamics. In order to facilitate this, we comprehensively develop the connection between cDFT energy derivatives and response functions, providing a rigorous assessment of the uniqueness and character of cDFT stationary points while accounting for electronic interactions and screening. In particular, we provide a new, non-perturbative proof that stable stationary points of linear density constraints occur only at energy maxima with respect to their Lagrange multipliers. We show that multiple solutions, hysteresis, and energy discontinuities may occur in cDFT. Expressions are derived, in terms of convenient by-products of cDFT optimization, for quantities such as the dielectric function and a condition number quantifying ill-definition in multi-constraint cDFT.

PACS numbers: 71.15.-m, 31.15.E-, 71.15.Qe, 71.15.Dx

I. BACKGROUND

Constrained density functional theory (cDFT)[1] is a generalization of density functional theory (DFT)[2,3] in which external constraints are applied in order to simulate excitation processes, to calculate response properties, or to impose a physical condition that is not met by the unconstrained approximate exchange-correlation functional. Such constraints may be applied to expectation values of the charge or spin density, their sums, differences, and moments within pre-defined spatial regions[4–16]. They are necessarily chosen on the basis of physical intuition and experience. Constraining potentials that are non-local or orbital-dependent may also be introduced, moving beyond formal DFT[4]. cDFT enables individual excited states to be studied within the well-established framework of ground-state DFT[4–7,17–19], particularly those excited states which may be represented as the ground-state for some potential. While these excitations are not guaranteed to match the neutral excitations of the system, yielded by time-dependent DFT[20], for example, their description may nonetheless benefit from physical conditions, such as charge transfer, which may be absent from the approximate functional but reintroduced using cDFT. As such, cDFT offers important insights that are challenging to obtain otherwise[5,11,17,21,22].

In practice, cDFT has proven to be a very efficient approach for simulating neutral excitations in molecular systems, particularly in cases where a clear spatial delineation may be made between charge (or spin) donor and acceptor regions[4–7,17–19,21–24]. cDFT is a significant asset, therefore, to the simulation of exciton formation, where the incorrect long-ranged behaviour of conventional local or semi-local exchange-correlation functionals may be partially corrected by using appropriately constructed constraints[19,23–26]. It has also been used to calculate electron transfer[11,27–36], excitation energy transfer[37,38], and exchange coupling parameters[14,15,39] for use in model Hamiltonians, as well as Coulomb interaction parameters for methods such as DFT+U[40–45]. Moreover, cDFT has been shown to provide an effective correction for the self-interaction error exhibited by approximate functionals when calculating diabatic free-energy surfaces for electron-transfer reactions[11]. As a promising antidote to static correlation error in approximate functionals, cDFT has been used to generate small, efficient basis sets for configuration interaction calculations, by enabling the most relevant charge and spin states to be straightforwardly sampled[22,46–49]. For a recent comprehensive review of cDFT, we refer the reader to Ref. 1.

cDFT may yet play unforeseen roles in future first-principles atomistic simulation. As the field moves increasingly towards the automated construction and interrogation of materials databases generated using high-throughput DFT approaches[50,51], for example, it could be used in the large-scale screening of candidate charge-transfer and energy-transfer materials or, as we describe below, to screen for the average local microscopic dielectric functions of complex materials and interfaces. In order for the great utility and potential of the cDFT approach to be fully and routinely realized in the simulation of charge-transfer excitations, and in degenerate or strongly-interacting systems, it must be efficiently automated, reliable, and convenient for users. For this, robust optimisation algorithms for the Lagrange-multipliers enforcing the constraint functionals of cDFT are desirable, and indeed necessary in cases of multiple simultaneous constraints being applied, such as on charge and spin[1,4,9,10,18]. Additionally, automated Lagrange multiplier updates at each ionic configuration are indispens-

able when performing geometry optimisation[4–7,17,18] or molecular dynamics[10,11,30,33,52] in tandem with cDFT.

Critical to both the theoretical underpinning and viability of cDFT optimization is the nature of the energy landscape with respect to the Lagrange multipliers that determine the strength of its constraining potentials. In particular, certainty about the nature and uniqueness of any stationary points at which the constraints are satisfied is a prerequisite to efficiently locating them numerically. Wu and Van Voorhis (W&VV)[5] carried out the pioneering and enabling work in this area, analysing the relevant derivatives, and their principal results have been subsequently synopsized in numerous works[1,4,18,24,53]. It was concluded by W&VV[5] on the basis of non-degenerate perturbation theory that a non-trivial stationary point, for an arbitrary constraint on the electron density, arises only at a maximum of the total-energy with respect to a cDFT Lagrange multiplier, and that this solution is unique. This is a central result in cDFT, suggesting the feasibility of its routine automated optimization, which has been extended to multivariate cases in Refs. 4 and 1.

II. INTRODUCTION AND MOTIVATION

In this work, we rigorously generalize the latter result, building upon the foundation provided by W&VV's cDFT stationary point classification, first showing that the analysis becomes inconclusive when electronic screening effects are considered. Specifically, we find that while the cDFT energy curvature[54] formula derived by W&VV is appropriate for updating cDFT Lagrange multipliers during the density update step, or inner loop, of self-consistent field DFT algorithms[4,55,56], it is not applicable to the self-consistently relaxed total-energy relevant to the global classification of cDFT solutions. Fig. 3 illustrates the large discrepancy between the cDFT energy curvatures calculated using W&VV's formula (solid circles) and those evaluated using finite-differences (open squares), hence the necessity to revisit the topic here.

In addition, Fig. 1 shows cDFT data that exhibits effects not hitherto discussed in the relevant literature, to our knowledge, namely multiple solutions, hysteresis, and energy discontinuities, and thus further motivates the present study. Here, the ONETEP linear-scaling simulation code[57], as discussed in Section IV, was used to carry out cDFT calculations on the hydrogen molecule stretched to an internuclear distance of 3.2 a_0, which, using the PBE functional[58] with no spin-orbit coupling, lies just beyond the Coulson-Fischer point at which an open-shell singlet ground-state becomes favoured[59,60]. A constraint was placed on the difference of spin magnetic moments, ΔM, between the two hydrogen atoms, defined on the basis of their isolated $1s$ valence pseudo-orbitals. The constraint target was set to $\Delta M_c = 0\ \mu_B$, and the Lagrange multiplier V_c was defined such that increasing its value increased the spin-dependent potential acting to decrease ΔM. It was found that the unpolarized, closed

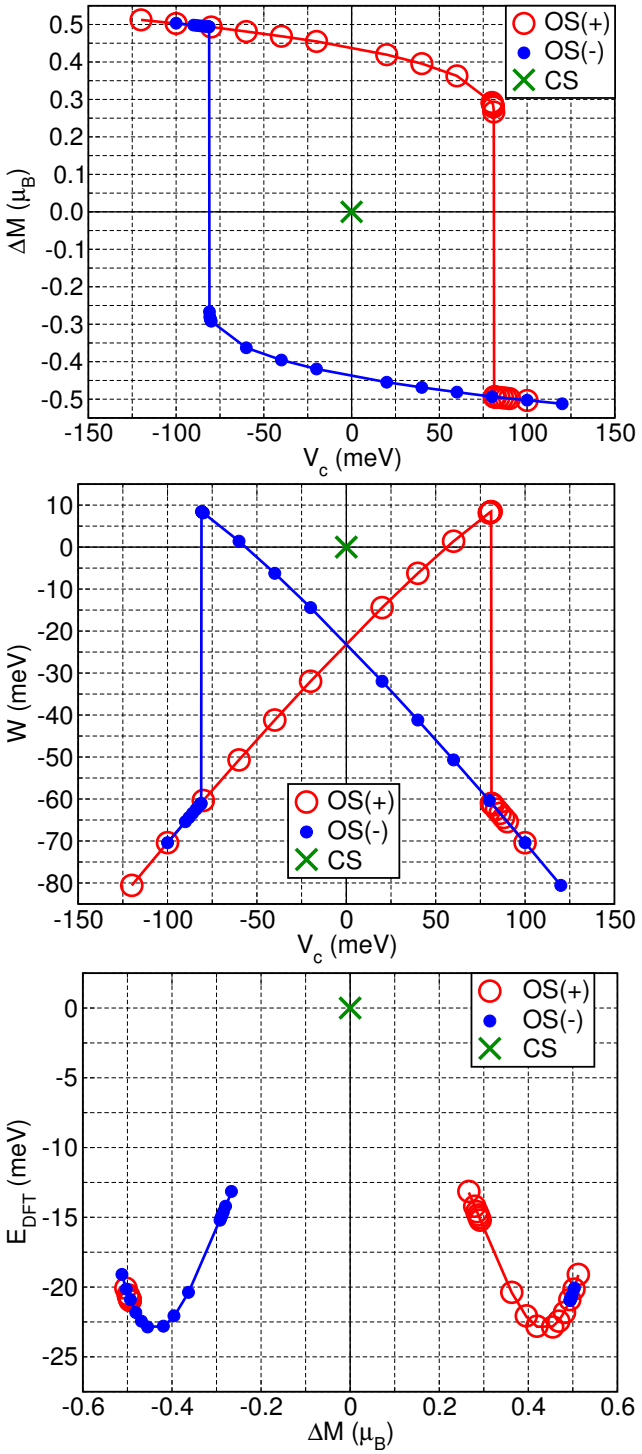

FIG. 1. (Color online) Multiple solutions and hysteresis in spin-constrained, open-shell, stretched molecular hydrogen. Shown are (top) the magnetic moment difference ΔM between constrained regions versus the Lagrange multiplier V_c, (middle) the cDFT total-energy W versus V_c corresponding to a target moment difference $\Delta M_c = 0\ \mu_B$, and (bottom) the DFT energy component E_{DFT} versus ΔM. "OS(-)" indicates data obtained using the open-shell ground-state with negative ΔM at ($V_c = 0$), "OS(+)" the symmetry-related open-shell solution with positive ΔM ($V_c = 0$), with data adapted from the latter, and "CS" the meta-stable closed-shell solution.

shell "CS" state is meta-stable, starting from which any non-zero value of V_c initiates a collapse to one of two symmetry-related, degenerate open-shell ground-states, "OS(-)" and "OS(+)" defined in the caption of Fig. 1.

The constraint proved capable of traversing between the two energy basins associated with these states (the "CS" state lies at the saddle point connecting them), insofar as that it caused abrupt switching between states at a critical constraining potential of $V_c \approx \pm 81.1$ meV. The top panel of Fig. 1 shows that multiple energy minima are possible for particular values of the cDFT Lagrange multiplier V_c, that certain ranges of the constraint target (in this case ΔM_c) may be inaccessible to cDFT, and that its response diverges simultaneously with an energy discontinuity at the transition between states. The middle panel shows that the total-energy W may exhibit non-differentiable cusps at such points, close to which cDFT optimisation is impracticable. The bottom panel shows the DFT contribution to the total-energy, E_{DFT}, as a function of the constrained quantity, and the two symmetry-related "OS" energy basins in question. Geometrically, it is inevitable that at least some solutions within the inaccessible interval connecting these two curves would, in principle, exhibit negative curvatures. We will show that such solutions, unless meta-stable like the "CS" state, are unstable due to anomalous response function sign, and thus cannot be realized using cDFT.

Prompted by these results, in the following we provide generalized energy curvature expressions which ensure that the stable stationary points of non-trivial linear constraints in the density may occur only at maxima of the total-energy with respect to their Lagrange multipliers, thereby cementing the theoretical basis of automated cDFT optimization. Our approach is general up to arbitrary orders in response and it also lifts the assumption of orbital non-degeneracy made in W&VV's treatment. It also allows for the maximizability of the cDFT energy to imply the uniqueness of such maxima only when the unconstrained system is devoid of multiple electronic minima, a specific counterexample of which is demonstrated by Fig 1. The consistency of our analytical approach is validated throughout this work by means of numerically verified equalities, in some cases newly established, between integrated linear-response functions and components of the cDFT total-energy curvature. As such, the present work represents a timely, comprehensive treatment of density response from the energy landscape perspective. We provide energy-curvature relationships for each of the integrated response and inverse-response functions, both interacting and non-interacting, which we generalize to multiple constraints.

These response functions are by-products of cDFT Lagrange multiplier optimization, and they can be used, for example, to calculate the average dielectric constant in a particular region, which is of critical importance for supercell convergence acceleration[19] and implicit solvation[61,62] schemes. A formula for the cDFT optimization condition number is provided, intended for identifying systems in which extremization of the cDFT total-energy is to be expected to present challenges, and in which Newton's method may be apposite, as has previously been suggested within the cDFT context in Refs. 1, 4, and 10.

Given the broad span of the physical and mathematical issues necessarily considered and revised, and to favor the readability of the article, it is organized into Sections, as follows. In Section III, we present and discuss the previously overlooked role of dielectric screening in the energy derivatives in self-consistent cDFT. In Section IV, we introduce the formal connections between the Lagrange multiplier curvature of the different contributions to the cDFT total-energy and the integrated electronic response function, both in the interacting and non-interacting cases. These newly derived formulae are then applied to globally characterize the stationary points of cDFT, both in the single constraint (Section V) and multiple constraint (Section VI) cases. In Section VII, we provide a synopsis of our main findings and conclusions.

III. DIELECTRIC SCREENING OF CONSTRAINED DFT ENERGY DERIVATIVES

We begin our analysis with the cDFT[1] constraint functional as per the definition and notation introduced in the founding article on cDFT automation by W&VV[5]. We consider an electronic system treated using Kohn-Sham density-functional theory (DFT)[2,3], subject to an arbitrary constraint on its electron density (see W&VV's Eq. 1, Ref. 8 and footnote[63]) of the linear form

$$C\left[\rho\right] = N\left[\rho\right] - N_c; \;\; N\left[\rho\right] = \sum_{\sigma} \int w_c^{\sigma}\left(\mathbf{r}\right) \rho^{\sigma}\left(\mathbf{r}\right) \, d\mathbf{r}. \quad (1)$$

Here, $\rho^{\sigma}\left(\mathbf{r}\right)$ is the electronic density of spin σ, $w_c^{\sigma}\left(\mathbf{r}\right)$ is an arbitrary local weight function describing a spatial region of particular interest in the system, and N_c is the target electron number to be enforced on that region. In order to apply this constraint, a term is added to the conventional DFT total-energy, $E_{\mathrm{DFT}}\left[\rho\right]$, to build the functional given by (c.f. W&VV's Eq. 4)

$$W\left[\rho, V_c\right] = E_c\left[\rho, V_c\right] + E_{\mathrm{DFT}}\left[\rho\right], \;\; \text{with} \quad (2)$$

$$E_c\left[\rho, V_c\right] = V_c C\left[\rho\right], \quad (3)$$

where V_c is the Lagrange multiplier. Minimizing W with respect to the density via the Kohn-Sham orbitals $\phi_{i\sigma}$, for a given V_c, under the condition that these orbitals are orthonormalized for each spin, gives rise to the Kohn-Sham equations[3] including a constraining potential $V_c w_c^{\sigma}\left(\mathbf{r}\right)$. This minimization, which is equivalent to solving the constrained Kohn-Sham equations, does not correspond to the free extremization $\delta W / \delta \phi_{i\sigma}^{*} = 0$ invoked by W&VV, since the functional derivative cannot encode the orbital orthonormality constraint. Rather, it

instead corresponds to extremizing the Lagrangian

$$\Omega\left[\rho,V_c\right]=W\left[\rho,V_c\right]-\sum_{\sigma}\sum_{ij}^{N_\sigma}\varepsilon_{ij\sigma}\left(\int\phi_{i\sigma}^{*}\left(\mathbf{r}\right)\phi_{j\sigma}\left(\mathbf{r}\right)\,d\mathbf{r}-\delta_{ij}\right). \tag{4}$$

Here, we have assumed that the system is Kohn-Sham insulating, for simplicity, with N^σ electrons per spin σ. Following application of the condition $\delta\Omega/\delta\phi_{i\sigma}^{*}=0$, we may perform a unitary transformation among the resulting equations. This also transforms the orbitals, yet it presents no difficulties since $\Omega\left[\rho,V_c\right]$ is invariant under such transformations for density functionals. Diagonalising the matrix Lagrange multiplier $\varepsilon_{ij\sigma}$, thereby, returns the Kohn-Sham cDFT equations of W&VV's Eq. 5, with eigenvalues $\varepsilon_{i\sigma}$. Thus, we may succinctly write, at the physically relevant minimum of W, the expression $\delta W/\delta\phi_{i\sigma}^{*}=\hat{H}_\sigma\phi_{i\sigma}$ or indeed its complex conjugate $\delta W/\delta\phi_{i\sigma}=\phi_{i\sigma}^{*}\hat{H}_\sigma$, where $\hat{H}_\sigma$ is the Kohn-Sham cDFT Hamiltonian for spin σ. Following W&VV, we may next define the function $W\left(V_c\right)$ as the evaluation of $W\left[\rho,V_c\right]$ using the density generated by the orthonormal orbitals which solve the Kohn-Sham equations including the constraining potential $V_c w_c^\sigma\left(\mathbf{r}\right)$ or, for the avoidance of doubt concerning Kohn-Sham excited states, as the physical minimum of the total-energy for a given V_c.

A. Total-energy first derivative

We now begin to analyze the derivatives of $W\left(V_c\right)$ required for the location of cDFT solutions. Partial derivatives couple only explicit dependencies, and are sufficient for optimising the Lagrange multiplier during the density update step, or inner loop, of self-consistent field DFT algorithms[4,56]. In order to determine the character of cDFT stationary points globally, on the other hand, we must consider total derivatives, which include orbital and density relaxation effects. In simulations where a number of constraints are simultaneously applied, their Lagrange multipliers are independent variables, so that the Hessian of interest is the matrix of mixed second total derivatives. These simulations are discussed in Section VI.

The first total derivative of the cDFT total-energy with respect to the Lagrange multiplier, V_c, is given by

$$\begin{aligned}\frac{dW}{dV_c}&=\sum_{\sigma}\sum_{i}^{N_\sigma}\mathrm{Tr}\left[\frac{\delta W}{\delta\phi_{i\sigma}^{*}}\frac{d\phi_{i\sigma}^{*}}{dV_c}+c.c.\right]+\frac{\partial W}{\partial V_c}\\&=\sum_{\sigma}\sum_{i}^{N_\sigma}\mathrm{Tr}\left[\left(\hat{H}_\sigma\phi_{i\sigma}\right)\frac{d\phi_{i\sigma}^{*}}{dV_c}+c.c.\right]\\&\quad+\left(\sum_{\sigma}\int w_c^\sigma\left(\mathbf{r}\right)\rho^\sigma\left(\mathbf{r}\right)\,d\mathbf{r}-N_c\right),\end{aligned} \tag{5}$$

where the trace symbol Tr denotes an integral over space since the operators are all local, and *c.c.* represents the complex conjugate of the preceding term. For any value of V_c, the orbitals that generate the density minimizing $\Omega\left[\rho,V_c\right]$ are unique up to unitary transformations, and we are free to choose the set that diagonalize the Hamiltonian. This allows us to simplify the latter expression, since it guarantees that the orbital-coupling term

$$\begin{aligned}\mathrm{Tr}\left[\left(\hat{H}_\sigma\phi_{i\sigma}\right)\frac{d\phi_{i\sigma}^{*}}{dV_c}\right]&=\varepsilon_{i\sigma}\mathrm{Tr}\left[\phi_{i\sigma}\frac{d\phi_{i\sigma}^{*}}{dV_c}\right]\\&=\varepsilon_{i\sigma}\int\phi_{i\sigma}\left(\mathbf{r}\right)\sum_{a\neq i}\phi_{a\sigma}^{*}\left(\mathbf{r}\right)\,d\mathbf{r}\\&\quad\times\int\frac{\phi_{a\sigma}^{*}\left(\mathbf{r}'\right)\frac{dv_\sigma^{\mathrm{KS}}\left(\mathbf{r}'\right)}{dV_c}\phi_{i\sigma}\left(\mathbf{r}'\right)}{\varepsilon_{i\sigma}-\varepsilon_{a\sigma}}\,d\mathbf{r}'\end{aligned} \tag{6}$$

evaluates to zero by virtue of the orthonormality of $\phi_{i\sigma}$ and $\phi_{a\sigma}$ for $a\neq i$. Here, v_σ^{KS} is the Kohn-Sham potential, i.e., the total effective potential which enters density-functional perturbation theory[64,65].

If focusing on the self-consistent field DFT inner loop as per W&VV, we may neglect screening effects and, thereby, assert that the change in total potential equals the external perturbation $\delta\hat{v}_\sigma^{\mathrm{external}}$, and then $\delta\hat{v}_\sigma^{\mathrm{KS}}=\delta\hat{v}_\sigma^{\mathrm{external}}=\hat{w}_c^\sigma\delta V_c$, whence $dv_\sigma^{\mathrm{KS}}\left(\mathbf{r}\right)/dV_c=\hat{w}_c^\sigma\left(\mathbf{r}\right)$ in the above expression. More generally, however, an account of electronic screening of the perturbation is necessary, and such effects are encapsulated in the inverse microscopic dielectric function defined by $\epsilon_{\sigma\sigma'}^{-1}\left(\mathbf{r},\mathbf{r}'\right)=dv_\sigma^{\mathrm{KS}}\left(\mathbf{r}\right)/dv_{\sigma'}^{\mathrm{external}}\left(\mathbf{r}'\right)$[66]. For pure (density-constrained rather than non-local) cDFT, we may write that

$$\begin{aligned}\frac{dv_\sigma^{\mathrm{KS}}\left(\mathbf{r}\right)}{dV_c}&=\sum_{\sigma'}\int\frac{dv_\sigma^{\mathrm{KS}}\left(\mathbf{r}\right)}{dv_{\sigma'}^{\mathrm{external}}\left(\mathbf{r}'\right)}\frac{dv_{\sigma'}^{\mathrm{external}}\left(\mathbf{r}'\right)}{dV_c}\,d\mathbf{r}'\\&=\sum_{\sigma'}\int\epsilon_{\sigma\sigma'}^{-1}\left(\mathbf{r},\mathbf{r}'\right)w_c^{\sigma'}\left(\mathbf{r}'\right)\,d\mathbf{r}'\\&\equiv\left(\epsilon^{-1}w_c\right)^\sigma\left(\mathbf{r}\right).\end{aligned} \tag{7}$$

For cDFT with non-local potentials, the symmetric form $\left(\epsilon^{-1/2}w_c\epsilon^{-1/2}\right)^\sigma\left(\mathbf{r},\mathbf{r}'\right)$ may be used in place of the latter in order to ensure that the potential remains Hermitian.

Screening effects notwithstanding, all cancels to zero in the total derivative of $W\left(V_c\right)$ except for the explicit constraint contribution on the final line of Eq. 5, namely $\partial W/\partial V_c=C$, which then evaluates to zero when the constraint is satisfied. Thus, the task of enforcing the constraint condition is transformed into that of locating the stationary points of W with respect to V_c. As an aside, this result mirrors W&VV's Eq. 6, which was derived in a slightly different way by invoking $\delta W/\delta\phi_{i\sigma}^{*}=0$ rather than $\delta W/\delta\phi_{i\sigma}^{*}=\hat{H}_\sigma\phi_{i\sigma}$, the numerical distinction between which is vanishing due to Kohn-Sham orbital orthonormality. Finally, we note that the vanishing trace in Eq. 5 may be partitioned into two contributions which

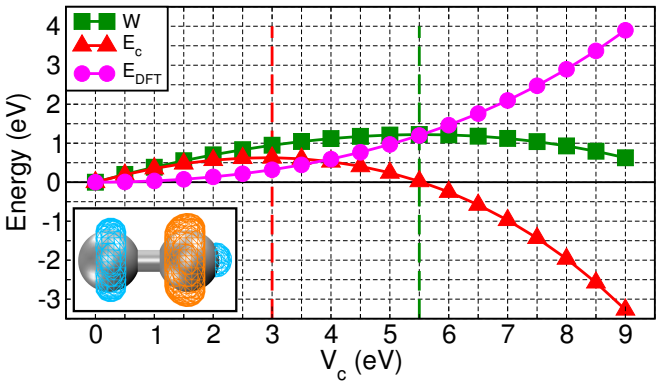

FIG. 2. (Color online) The cDFT total-energy W, and its constraint, E_c, and DFT, E_{DFT}, components, as a function of the Lagrange multiplier V_c, for a charge-constrained nitrogen molecule. The V_c values for the data points at which E_c and W attain maxima are shown with dashed vertical red and green lines, respectively. Inset: the left-hand atom is constrained to lose charge with respect to its ground-state population, using an on-atom population analysis combining s and p orbitals. With respect to the ground-state density, charge depleted regions are shown with a cyan charge-difference isosurface and the charge augmented region is shown with an orange isosurface. The unconstrained right-hand atom exhibits strong polarization, and depletion in the lone-pair region.

cancel, for any value of V_c, by means of the expression

$$\frac{\delta W}{\delta\phi^*_{i\sigma}} = \frac{\delta E_c}{\delta\phi^*_{i\sigma}} + \frac{\delta E_{\mathrm{DFT}}}{\delta\phi^*_{i\sigma}} = V_c\frac{\delta C}{\delta\phi^*_{i\sigma}} + \frac{\delta E_{\mathrm{DFT}}}{\delta\phi^*_{i\sigma}}$$
$$\Rightarrow \quad 0 = V_c\mathrm{Tr}\left[\frac{\delta C}{\delta\phi^*_{i\sigma}}\frac{d\phi^*_{i\sigma}}{dV_c}\right] + \mathrm{Tr}\left[\frac{\delta E_{\mathrm{DFT}}}{\delta\phi^*_{i\sigma}}\frac{d\phi^*_{i\sigma}}{dV_c}\right]. \quad (8)$$

Thus, both the DFT energy E_{DFT} and the constraint energy E_c may individually contribute substantially to the derivatives of $W(V_c)$, as shown in Fig. 2. As a result, a stationary total-energy W with respect to the cDFT Lagrange multiplier does not imply a stationary constraint contribution E_c alone, and vice versa.

B. Total-energy second derivative by means of non-degenerate perturbation theory

The second derivative or "curvature" of $W(V_c)$, is required to classify any stationary point, or points, at which the constraint is satisfied. In cases where the second derivative vanishes, higher derivatives may also be needed. We consider here the self-consistent cDFT energy landscape, rather than the unscreened problem specific to the inner loop of self-consistent field DFT codes[4,55,56], and the resulting curvature differs from that of W&VV's treatment in magnitude and, potentially, in sign. Following from Eq. 5 and applying the product rule for differentiation where necessary, we may write that

$$\begin{aligned}\frac{d^2W}{dV_c^2} &= \frac{d}{dV_c}\sum_\sigma\sum_i^{N_\sigma}\mathrm{Tr}\left[\left(\hat{H}_\sigma\phi_{i\sigma}\right)\frac{d\phi^*_{i\sigma}}{dV_c} + c.c.\right] + \frac{dC}{dV_c}\\
&= \sum_\sigma\sum_i^{N_\sigma}\mathrm{Tr}\left[\left(\frac{d\hat{H}_\sigma}{dV_c}\phi_{i\sigma}\right)\frac{d\phi^*_{i\sigma}}{dV_c} + c.c.\right]\\
&\quad + \sum_\sigma\sum_i^{N_\sigma}\mathrm{Tr}\left[\left(\hat{H}_\sigma\frac{d\phi_{i\sigma}}{dV_c}\right)\frac{d\phi^*_{i\sigma}}{dV_c} + c.c.\right]\\
&\quad + \sum_\sigma\sum_i^{N_\sigma}\mathrm{Tr}\left[\left(\hat{H}_\sigma\phi_{i\sigma}\right)\frac{d^2\phi^*_{i\sigma}}{dV_c^2} + c.c.\right]\\
&\quad + \sum_\sigma\int w_c^\sigma(\mathbf{r})\frac{d\rho^\sigma(\mathbf{r})}{dV_c}\,d\mathbf{r}. \quad (9)\end{aligned}$$

This makes the contributions arising at second order in perturbation theory explicit. These rather cumbersome terms may be circumvented by noting that the eigencondition $\hat{H}_\sigma\phi_{i\sigma} = \varepsilon_{i\sigma}\phi_{i\sigma}$ holds continuously as we vary the parameter V_c. As a result, the quantity expressed in Eq. 6 vanishes for all V_c, and so we may write that

$$\frac{d}{dV_c}\mathrm{Tr}\left[\left(\hat{H}_\sigma\phi_{i\sigma}\right)\frac{d\phi^*_{i\sigma}}{dV_c}\right] = 0. \quad (10)$$

Thus, all terms in Eq. 9 numerically cancel except for the final term, dC/dV_c. This may then be re-written using non-degenerate (only where applicable) first-order perturbation theory, after the present Eq. 6, since

$$\begin{aligned}\frac{dC}{dV_c} &= \frac{d}{dV_c}\sum_\sigma\int w_c^\sigma(\mathbf{r})\,\rho^\sigma(\mathbf{r})\;d\mathbf{r}\\
&= \sum_\sigma\sum_i^{N_\sigma}\int w_c^\sigma(\mathbf{r})\,\phi^*_{i\sigma}(\mathbf{r})\frac{d\phi_{i\sigma}(\mathbf{r})}{dV_c}\,d\mathbf{r} + c.c.\\
&= \sum_\sigma\sum_i^{N_\sigma}\int w_c^\sigma(\mathbf{r}')\,\phi^*_{i\sigma}(\mathbf{r})\sum_{a\neq i}\phi_{a\sigma}(\mathbf{r})\;d\mathbf{r}\\
&\quad\times\int\frac{\phi^*_{a\sigma}(\mathbf{r}')\frac{dv_\sigma^{\mathrm{KS}}(\mathbf{r}')}{dV_c}\phi_{i\sigma}(\mathbf{r}')}{\varepsilon_{i\sigma}-\varepsilon_{a\sigma}}\,d\mathbf{r}' + c.c.\\
&= \sum_\sigma\sum_i^{N_\sigma}\sum_{a\neq i}\frac{1}{\varepsilon_{i\sigma}-\varepsilon_{a\sigma}}\\
&\quad\times\left(\left(\int\phi^*_{a\sigma}(\mathbf{r})\,w_c^\sigma(\mathbf{r})\,\phi_{i\sigma}(\mathbf{r})\;d\mathbf{r}\right)\right. \quad (11)\\
&\quad\left.\times\left(\int\phi^*_{i\sigma}(\mathbf{r}')\left(\varepsilon^{-1}w_c\right)^\sigma(\mathbf{r}')\,\phi_{a\sigma}(\mathbf{r}')\;d\mathbf{r}'\right)\right) + c.c..\end{aligned}$$

The latter expression reduces to W&VV's Eq. 7 if screening effects are neglected, that is if we set $\varepsilon^{-1}_{\sigma\sigma'}(\mathbf{r},\mathbf{r}') = \delta_{\sigma\sigma'}\delta(\mathbf{r}-\mathbf{r}')$. Then, as noted by W&VV, the antisymmetry of the summand implies both that contributions from $a \leq N_\sigma$ cancel to zero and may be omitted, and that the total is strictly non-positive. This condition holds in non-degenerate, linearly-responding cases

of cDFT Lagrange multiplier optimisation carried out within the potential-update loop of self-consistent field DFT codes, where W&VV's result ensures the sign of the energy curvature for any fixed Kohn-Sham potential.

Globally speaking, however, it appears that the sign of the energy curvature cannot be inferred directly from the symmetries of Eq. 11. The necessarily real-valued screened weight function $\left(\varepsilon^{-1}w_c\right)^{\sigma}(\mathbf{r})$ may locally vary, even in sign, with respect to $w_c(\mathbf{r})$, in a complex, system-dependent manner, typically causing an average net attenuation of the constraining potential. Even if we may assume that $0 < \left(\varepsilon^{-1}w_c\right)^{\sigma}(\mathbf{r}) < w_c(\mathbf{r})$ holds everywhere, for a particular system, and that the orbitals are filled according to the Aufbau principle in Eq. 11, the form of this sum offers no guarantee regarding the sign of d^2W/dV_c^2.

On the other hand, experience and extensive literature (see review Ref. 1) yield observations that d^2W/dV_c^2 is negative for density constraints applied to a wide variety of systems. As now we go on to numerically confirm, Eq. 10 provides that this curvature reduces, for ground-states, to the interacting density response function of the system, doubly integrated with w_c^{σ}. On this basis, we will show in Section V that any solutions of non-negative curvature are meta-stable (e.g., the "CS" state of Fig. 1) or unstable (e.g., the inaccessible region in the vicinity of "CS") with respect to small perturbations, so that such curvatures cannot be directly computed and plotted.

The presence of the inverse microscopic dielectric function in Eq. 11 renders it unsuitable for use in accelerating the convergence of automated cDFT Lagrange multiplier optimization. Even by using a finite-difference method for Eq. 7, or indeed in the absence of screening effects, a converged sum over unoccupied states at each cDFT Lagrange multiplier optimization step is computationally demanding and conceptually undesirable in DFT. To overcome these drawbacks, in the following Section we present an alternative approach for characterizing cDFT energy curvatures, in the framework of response theory.

IV. CDFT ENERGY CURVATURES FROM THE RESPONSE FUNCTION PERSPECTIVE

As an alternative to classifying the cDFT energy landscape by means of summation over unoccupied states, in what follows we express the relevant energy curvatures in terms of more computationally convenient integrated response functions, which depend only on the density or occupied states. This Section is intended to provide a comprehensive treatment of the relationship between density response functions and energies in cDFT. We extend our principal results to the multivariate regime of multiple simultaneous constraints in Section VI. These response functions are convenient by-products of automated cDFT optimization, and they are experimental observables in simulations where the constraining potentials are those of physical fields. For a cDFT potential representing a uniform electric field, for example, $w_c^{\sigma}(\mathbf{r})$ has a constant

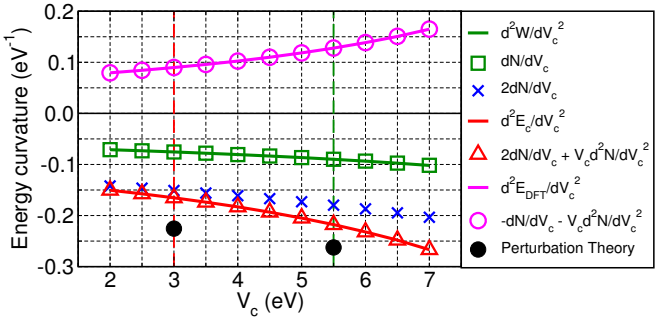

FIG. 3. (Color online) The numerically evaluated curvature (second derivatives) of the cDFT total-energy W, and its constraint, E_c, and DFT, E_{DFT}, components, with respect to the Lagrange multiplier, V_c, for the system shown in Fig. 2. Dashed vertical lines have the same significance as in Fig. 2. The Lagrange multiplier derivatives of the constrained occupancy N, which correspond to the latter curvatures, are shown, as well as the linear-response approximation to one of them (crosses). Evaluated values of the unscreened sum-over-states perturbation theory expression for d^2W/dV_c^2, following W&VV, are also shown (solid circles).

gradient, and the integrated interacting response function represents the high-frequency electric dipole-dipole polarizability α_{∞}. Another example is the microscopic dielectric constant averaged over a region, which is an important ingredient for supercell convergence acceleration[19] and implicit solvation[61,62] schemes. The results provided below allow such response functions to be calculated, and even updated in self-consistent schemes.

A. The integrated interacting response function

The interacting linear response function $\chi^{\sigma\sigma'}(\mathbf{r},\mathbf{r}')$ measures the response in the density due to a small change in the applied potential. Since, by definition,

$$\begin{aligned} d\rho^{\sigma}(\mathbf{r}) &= \int \chi^{\sigma\sigma'}(\mathbf{r},\mathbf{r}')\, dv_{\sigma'}^{\text{external}}(\mathbf{r}')\; d\mathbf{r}' \\ &= \sum_{\sigma'} \int \chi^{\sigma\sigma'}(\mathbf{r},\mathbf{r}')\, w_c^{\sigma'}(\mathbf{r}')\, dV_c^{\sigma'}\; d\mathbf{r}', \end{aligned} \tag{12}$$

one further integration over $w_c^{\sigma}(\mathbf{r})\, d\mathbf{r}$ allows us to define the integrated interacting density response function as

$$\begin{aligned} \chi^{\sigma\sigma'} &\equiv \iint w_c^{\sigma}(\mathbf{r})\, \chi^{\sigma\sigma'}(\mathbf{r},\mathbf{r}')\, w_c^{\sigma'}(\mathbf{r}')\, d\mathbf{r}\, d\mathbf{r}' \\ &= \frac{dN^{\sigma}}{dV_c^{\sigma'}} = \frac{d\int w_c^{\sigma}(\mathbf{r})\,\rho^{\sigma}(\mathbf{r})\; d\mathbf{r}}{d\int w_c^{\sigma'}(\mathbf{r}')\, V_c^{\sigma'}\; d\mathbf{r}'} \int w_c^{\sigma'}(\mathbf{r}'')\; d\mathbf{r}'', \end{aligned} \tag{13}$$

where we have made it explicit that dV_c is the average change in external potential over the subspace. For constraints defined using more general measures of the density or density matrix, such expressions may be generalised straightforwardly by replacing the local weighting functions $w_c^{\sigma}(\mathbf{r})$ by non-local projection operators.

The orthonormality preservation condition expressed in Eq. 10 guarantees the simplification of Eq. 9 to Eq. 11 for all values of V_c, and so provides that

$$\frac{d^2W}{dV_c^2} = \frac{dC}{dV_c} = \frac{dN}{dV_c} \equiv \chi = \frac{1}{2}\sum_{\sigma\sigma'} \chi^{\sigma\sigma'}, \qquad (14)$$

where the 1/2 is specific to collinear spins. Taking the constraint contribution alone, on the other hand, we find that the second-order response function survives, since

$$\begin{aligned}\frac{d^2E_c}{dV_c^2} &= \frac{d^2\left(V_cC\right)}{dV_c^2} = \frac{d}{dV_c}\left[C + V_c\frac{dC}{dV_c}\right] \\ &= 2\frac{dN}{dV_c} + V_c\frac{d^2N}{dV_c^2} = 2\chi + V_c\frac{d\chi}{dV_c}. \end{aligned} \qquad (15)$$

Combining these two results, we deduce a general result for the DFT energy component curvature, given by

$$\frac{d^2E_{\mathrm{DFT}}}{dV_c^2} = \frac{d^2\left(W - E_c\right)}{dV_c^2} = -\chi - V_c\frac{d\chi}{dV_c}. \qquad (16)$$

In order to check the validity of our approach for analyzing functional interdependencies and derivatives, and to numerically illustrate our analytical findings, we performed a cDFT study on the nitrogen molecule shown in Fig. 2. This serves to illustrate a case in which, if the constraint energy E_c vanishes for a finite Lagrange multiplier V_c, the total-energy W achieves a maximum with respect to V_c. The total and constraint energies W and E_c exhibit different negative curvatures, and their the difference, the DFT component E_{DFT}, necessarily exhibits a positive curvature around the ground-state minimum at $V_c = 0$ eV. For each value of the charge-constraining Lagrange multiplier, well converged BLYP[67,68] ground-state energies and densities, with pseudized 1s states, were calculated using the ONETEP linear-scaling Kohn-Sham DFT code[57]. This code solves for the ground-state by optimising a minimal set of nonorthogonal generalized Wannier functions[69] in situ. Each of these functions is expanded in an underlying variational plane-wave equivalent basis set and truncated within a prescribed cut-off sphere, in this particular case to a radius of 10 a_0. This approach has been shown to offer finite-difference linear response properties with an accuracy matching that of conventional plane-wave DFT[70]. The constrained population was defined using the four 2s and 2p valence pseudo-orbitals of the isolated atom[71]. In the dimer, the resulting unconstrained ground state atomic occupancy was approximately 6.5 e, due to overlap between pseudo-orbitals. The charge of one of the nitrogen atoms was constrained, with the target occupancy set to $N_c = 6.0$ e.

In Fig. 3, we note a very precise numerical correspondence between the total-energy curvature, its constraint, and DFT components, and their respectively predicted reformulations in terms of first and second order integrated interacting response functions, $\chi = dN/dV_c$ and $d\chi/dV_c$. This serves to confirm that the orthonormality preservation condition of Eq. 10 holds for all V_c. The failure of the linear-response approximation $2\chi = 2dN/dV_c$ (shown with blue crosses) to d^2E_c/dV_c is somewhat discouraging for the application of root-finding algorithms on E_c in order to optimize the cDFT potential, otherwise a plausible alternative or compliment to extremizing W.

Calculated values for the unscreened sum-over-states perturbation theory result for d^2W/dV_c^2 following W&VV, corresponding to the omission of screening in Eq. 11, are also shown in Fig. 3 (solid circles). For this, we generated optimized conduction band states using the method described in Ref. 72, with the conduction band Wannier function cutoff radii set to 14 a_0. This enabled us to numerically confirm that unscreened perturbation theory does not generally match the self-consistent total energy curvature, nor that of its constraint or DFT energy contributions individually. The anti-symmetry of the unscreened summand guarantees that it monotonically decreases with an increasing number of conduction band states, so that the difference between the measured energy curvature and the unscreened sum-over-states also monotonically increases with the number of states.

B. The integrated non-interacting response function and dielectric function

In Figs 4 and 5, we illustrate the relationship between energy curvatures and integrated density response functions with respect to the screened equivalent of the cDFT Lagrange multiplier, that is the average change in the Kohn-Sham potential over the constrained region. This provides a test of the magnitude and potential importance of dielectric screening effects in the energy versus Lagrange multiplier derivatives of self-consistent cDFT. The relevant weighted measure of the screened potential, for pure density functionals and constraints, is given by

$$V^{\sigma} = \left(\int w_c^{\sigma}\left(\mathbf{r}\right) v_{\sigma}^{\mathrm{KS}}\left(\mathbf{r}\right)\, d\mathbf{r}\right)\left(\int w_c^{\sigma}\left(\mathbf{r}'\right)\, d\mathbf{r}'\right)^{-1}. \qquad (17)$$

Then, whereas $\chi = dN/dV_c$ is the integrated interacting density response function, we may define $\chi_0 = dN/dV$ as its non-interacting (also known as independent-particle) counterpart. If $\chi_0^{\sigma\sigma'}\left(\mathbf{r},\mathbf{r}'\right) = d\rho^{\sigma}\left(\mathbf{r}\right)/dv_{\sigma}^{\mathrm{KS}}\left(\mathbf{r}'\right)$, then

$$\begin{aligned}\chi_0^{\sigma\sigma'} &= \frac{dN^{\sigma}}{dV^{\sigma'}} = \frac{d\int w_c^{\sigma}\left(\mathbf{r}\right)\rho^{\sigma}\left(\mathbf{r}\right)\, d\mathbf{r}}{d\int w_c^{\sigma'}\left(\mathbf{r}'\right) v_{\sigma'}^{\mathrm{KS}}\left(\mathbf{r}'\right)\, d\mathbf{r}'}\int w_c^{\sigma'}\left(\mathbf{r}''\right)\, d\mathbf{r}'' \\ &\approx \iint w_c^{\sigma}\left(\mathbf{r}\right)\chi_0^{\sigma\sigma'}\left(\mathbf{r},\mathbf{r}'\right) w_c^{\sigma'}\left(\mathbf{r}'\right)\, d\mathbf{r}\, d\mathbf{r}', \end{aligned} \qquad (18)$$

where the final approximation, a consequence of neglected local-field effects, becomes an equality in the special case that $w_c^{\sigma}\left(\mathbf{r}\right) dv_{\sigma}^{\mathrm{KS}}\left(\mathbf{r}\right) = w_c^{\sigma}\left(\mathbf{r}\right) dV$ for all $\mathbf{r}$.

Fig. 4 shows that replacing V_c by V does not preserve any equivalence between energy curvatures and response functions. Mixed derivatives with respect to V_c and V, the results of which are shown in Fig. 5, are required

for consistency of screening. Firstly, returning with the result $dW/dV_c = C$ for orthonormal states, we find that

$$\frac{d^2W}{dV\,dV_c} = \frac{dC}{dV} = \frac{dN}{dV} \equiv \chi_0 = \frac{1}{2}\sum_{\sigma\sigma'} \chi_0^{\sigma\sigma'}, \qquad (19)$$

which is numerically confirmed via Fig. 5. Next, we have

$$\begin{aligned}\frac{d^2E_c}{dV\,dV_c} &= \frac{d^2\left(V_cC\right)}{dV\,dV_c} = \frac{d}{dV}\left[C + V_c\frac{dC}{dV_c}\right] \\ &= \frac{dC}{dV} + \frac{dV_c}{dV}\frac{dC}{dV_c} + V_c\frac{d^2C}{dV\,dV_c} \\ &= 2\frac{dN}{dV} + V_c\frac{d^2N}{dV\,dV_c} = 2\chi_0 + V_c\frac{d\chi_0}{dV_c}, \end{aligned} \qquad (20)$$

since the derivatives with respect to the external and internal potentials commute. Finally, for the DFT component of the total-energy, we deduce that

$$\begin{aligned}\frac{d^2E_{\rm DFT}}{dV\,dV_c} &= \frac{d^2\left(W - E_c\right)}{dV\,dV_c} = -\frac{dN}{dV} - V_c\frac{d^2N}{dV\,dV_c} \\ &= -\chi_0 - V_c\frac{d\chi}{dV} = -\chi_0 - V_c\frac{d\chi_0}{dV_c}. \end{aligned} \qquad (21)$$

In practice, these mixed derivatives are calculated simultaneously with the previously detailed curvatures with respect to V_c, by monitoring the variation of the weighted, fully relaxed Kohn-Sham potential of Eq. 17 in self-consistent cDFT calculations. As before, we observe a precise agreement between the numerically evaluated energy curvatures and response functions. This confirms Eq. 19, namely, that the averaged non-interacting (i.e., independent-particle) response function of DFT may be expressed as an total-energy landscape property. We return to discuss the unscreened sum-over-states perturbation theory results shown in Figs. 4 and 5 in Appendix A.

The process of Lagrange multiplier optimization offers ready access to the physical response properties of the constrained region, which are not limited to those of the target state. The simplest such quantity is the subspace inverse dielectric constant (i.e., screening factor),

$$\begin{aligned}\epsilon^{-1}_{\sigma\sigma'} \equiv & \iint w_c^{\sigma}\left(\mathbf{r}\right)\epsilon^{-1}_{\sigma\sigma'}\left(\mathbf{r},\mathbf{r}'\right)w_c^{\sigma'}\left(\mathbf{r}'\right)\,d\mathbf{r}\,d\mathbf{r}' \\ & \times\left(\int w_c^{\sigma'}\left(\mathbf{r}''\right)\,d\mathbf{r}''\right)^{-1}. \end{aligned} \qquad (22)$$

This may be calculated directly using the cDFT integrated response functions, since, by definition,

$$\begin{aligned} dv_{\sigma}^{\rm KS}\left(\mathbf{r}\right) &= \int \epsilon^{-1}_{\sigma\sigma'}\left(\mathbf{r},\mathbf{r}'\right)dv_{\sigma'}^{\rm external}\left(\mathbf{r}'\right)\,d\mathbf{r}' \\ &= \int \epsilon^{-1}_{\sigma\sigma'}\left(\mathbf{r},\mathbf{r}'\right)w_c^{\sigma'}\left(\mathbf{r}'\right)dV_c^{\sigma'}\,d\mathbf{r}' \\ \Rightarrow \quad dV^{\sigma} &= \epsilon^{-1}_{\sigma\sigma'}dV_c^{\sigma'}. \end{aligned} \qquad (23)$$

From this, it is clear that $\epsilon^{-1}_{\sigma\sigma'}$ is a property of the constrained ground-state density and is not explicitly dependent on unoccupied states. Next, we may apply the chain rule via the the constrained property N^{σ}, introducing the notation $\chi_0^{-1\sigma\sigma''} = dV^{\sigma}/dN^{\sigma''}$, which provides that

$$\epsilon^{-1}_{\sigma\sigma'} = \frac{dV^{\sigma}}{dV_c^{\sigma'}} = \sum_{\sigma''}\chi_0^{-1\sigma\sigma''}\chi^{\sigma''\sigma'}. \qquad (24)$$

The inverse of this quantity is the subspace-averaged dielectric constant, neglecting local-field effects, given by

$$\epsilon_{\sigma\sigma'} = \frac{dV_c^{\sigma'}}{dV^{\sigma}} = \sum_{\sigma''}\chi_0^{\sigma\sigma''}\chi^{-1\sigma''\sigma'}. \qquad (25)$$

cDFT thus provides an efficient means of estimating the dielectric constants of spatial regions, which are central in implicit solvation[61,62], supercell convergence acceleration of excitation energies[19], and in high-frequency optical response, in terms of by-products of its optimization.

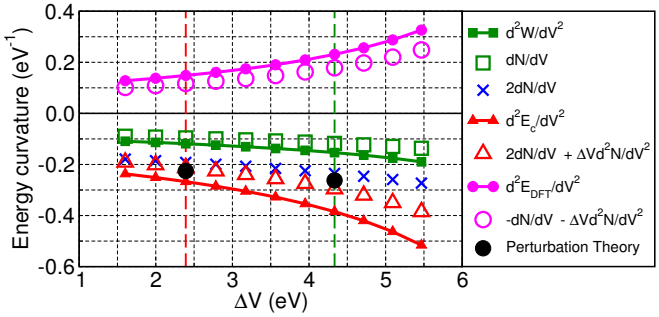

FIG. 4. (Color online) Results of the calculations shown in Fig. 3, where derivatives are instead taken with respect to the change in Kohn-Sham potential averaged over the constrained region, that is the ΔV induced by a finite V_c, using the same weight function as used to calculate the constrained occupancy N. The derivative dN/dV corresponds to the average non-interacting charge response of the constrained region, whereas dN/dV_c is the interacting response. Unlike the derivatives shown in Fig. 3, these non-interacting (i.e., bare or independent-particle) derivatives demonstrate no equivalence. The perturbation theory data points are as in Fig. 3.

V. STABLE CDFT SOLUTIONS ARE ENERGY MAXIMA WITH RESPECT TO THEIR LAGRANGE MULTIPLIER

The response function based approach to cDFT analysis is used in this Section to globally characterize its stationary points. W&VV have shown that a non-negative total-energy curvature with respect to the cDFT Lagrange multiplier is guaranteed in cases where non-degenerate perturbation theory is applicable[5], in the absence of screening effects. This regime may hold during cDFT optimization within the density-update loop of self-consistent field codes, where the Kohn-Sham potential is fixed[4,56]. More generally, or physically, the Kohn-Sham potential is relaxed self-consistently for each

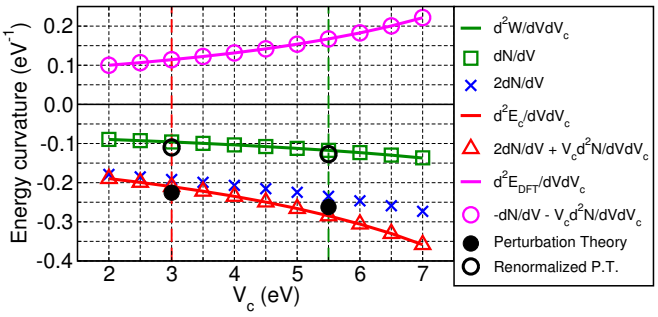

FIG. 5. (Color online) Following from Fig. 4, the correspondence between energy curvatures and averaged non-interacting response functions is recovered by using mixed interacting and non-interacting second derivatives, which restores their consistency. The sum-over-states perturbation theory (P.T.) data points following W&VV are again shown (solid circles), together with the "Renormalized P.T." data points (open black circles) described in Appendix A.

V_c, and sum-over-states perturbation theory becomes inconclusive as discussed in the text surrounding Eq. 11. We provide a general, non-perturbative proof that stable cDFT solutions always occur at energy maxima with respect to their Lagrange multiplier. We then extend this proof to the multivariate cDFT regime in Section VI.

We have shown that the curvatures of the total-energy with respect to the cDFT Lagrange multiplier V_c are equal to integrated density response functions. Next, we will show that, similarly, the curvatures with respect to the cDFT occupancy N, for a particular target N_c, are equal to the inverses of these response functions. The occupancy N is not a free parameter, and so, in order to analyze these curvatures, it is convenient to initially take derivatives with respect to the cDFT target occupancy N_c, subject to the condition that $N = N_c$ for a suitable Lagrange multiplier $V_c(N_c)$. Echoing Eq. 5, assuming that the ground-state is located for all V_c,

$$\begin{aligned}\frac{dW}{dN_c} &= \sum_\sigma \sum_i^{N_\sigma} \mathrm{Tr}\left[\left(\frac{\delta W}{\delta\phi^*_{i\sigma}}\frac{d\phi^*_{i\sigma}}{dV_c} + c.c.\right)\frac{dV_c}{dN_c}\right] + \frac{\partial W}{\partial N_c} \\ &= \sum_\sigma \sum_i^{N_\sigma} \mathrm{Tr}\left[\left(\left(\hat{H}_\sigma\phi_{i\sigma}\right)\frac{d\phi^*_{i\sigma}}{dV_c} + c.c.\right)\frac{dV_c}{dN_c}\right] - V_c \\ &= -V_c(N_c) \quad \Rightarrow \quad \frac{d^2W(N_c)}{dN_c^2} = -\frac{dV_c}{dN_c}. \end{aligned} \tag{26}$$

Since the constraint $N = N_c$ is satisfied for each N_c, the constraint energy always vanishes and $E_{\mathrm{DFT}}(N) = W(V_c(N_c))$ along the curve. Thus, we may write, for the occupancy curvature of the DFT contribution, that

$$\frac{d^2E_{\mathrm{DFT}}(N)}{dN^2} = \frac{d^2W(V_c(N_c))}{dN_c^2} = -\frac{dV_c}{dN} = -\chi^{-1}. \tag{27}$$

As previously established by W&VV for the unscreened case[5], the combination of Eqs. 14 and 27 provides that the curvature of the total-energy with respect to Lagrange multiplier is directly related to the curvature of the DFT energy with respect to the occupancy, namely

$$\begin{aligned}\left(\frac{d^2W}{dV_c^2}\right)^{-1} &= \left(\frac{dN}{dV_c}\right)^{-1} = \chi^{-1} \\ &= \frac{dV_c}{dN} = -\frac{d^2E_{\mathrm{DFT}}}{dN^2}. \end{aligned} \tag{28}$$

We may extend Eq. 28 to the general cDFT total-energy W, no longer subject the constraint that the target occupancy is attained, by freeing the target N_c after optimization of V_c. This has no bearing on E_{DFT}, by definition, and so Eq. 27 holds irrespective of whether the constraint is satisfied. For $W(V_c)$ with N not necessarily equal to N_c, it is sufficient to add the curvature of the now non-vanishing constraint energy term E_c, given by

$$\begin{aligned}\frac{d^2E_c}{dN^2} &= \frac{d^2(V_cC)}{dN^2} = \frac{d}{dN}\left[V_c\frac{dC}{dN} + C\frac{dV_c}{dN}\right] \\ &= 2\frac{dV_c}{dN}\frac{dC}{dN} + C\frac{d^2V_c}{dN^2} = 2\frac{dV_c}{dN} + (N-N_c)\frac{d^2V_c}{dN^2}. \end{aligned} \tag{29}$$

The total-energy curvature is provided by the sum

$$\begin{aligned}\frac{d^2W}{dN^2} &= \frac{d^2E_{\mathrm{DFT}}}{dN^2} + \frac{d^2E_c}{dN^2} \\ &= \frac{dV_c}{dN} + (N-N_c)\frac{d^2V_c}{dN^2}. \end{aligned} \tag{30}$$

Then, by combining Eqs. 27 to 30 and by applying the constraint condition $N = N_c$, we arrive at our central result that, valid for all cDFT stationary points as defined,

$$\left(\frac{d^2W}{dV_c^2}\right)^{-1} = \frac{1}{2}\frac{d^2E_c}{dN^2} = -\frac{d^2E_{\mathrm{DFT}}}{dN^2} = \frac{d^2W}{dN^2}. \tag{31}$$

This is numerically confirmed via Figs. 3 and 6, and the inaccuracy of linear-response approximations in Fig. 6 (shown with crosses), except at $N = N_c$, is clear.

Next, let us consider the possibility of simulating a stable constrained ground-state at a given value of V_c, which may be a cDFT solution but is not necessarily so. Stability implies that the energy is minimized with respect to the density, locally at least, and put more precisely, that the energy is locally strictly convex. Mathematically, this condition is represented by a positive definite matrix $d^2W/d\rho^{\sigma'}(\mathbf{r}')\,d\rho^{\sigma}(\mathbf{r})$, evaluated at a fixed V_c, where the coordinate pairs $\{\sigma, \mathbf{r}\}$ form the basis vectors. Separating the DFT and constraint energy terms, the stability of constrained ground-states is then determined by

$$\left.\frac{d^2W}{d\rho^{\sigma'}(\mathbf{r}')\,d\rho^{\sigma}(\mathbf{r})}\right|_{V_c,\hat{w}_c} = \frac{d^2E_{\mathrm{DFT}}}{d\rho^{\sigma'}(\mathbf{r}')\,d\rho^{\sigma}(\mathbf{r})}, \tag{32}$$

so that the latter is also positive definite. The underlying DFT energy landscape therefore alone determines the stability of constrained ground-states and thus, while cDFT may relocate the minima of W within the simply

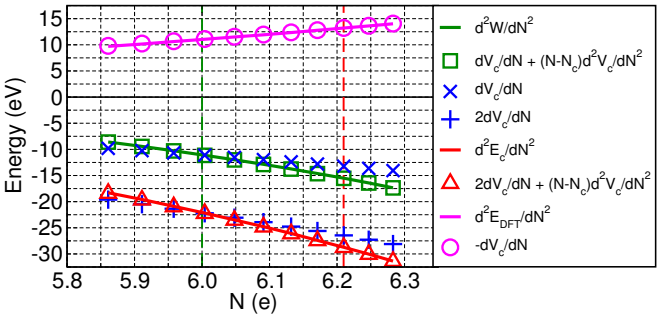

FIG. 6. (Color online) Numerically evaluated second derivatives of the cDFT total-energy W, its constraint E_c and DFT $E_{\rm DFT}$ components, with respect to the constrained occupancy N, for the system shown in Fig. 2 and occupancy target $N_c = 6$ e. Dashed vertical lines show the occupancy at which W (green) and E_c (red) are maximized. The corresponding occupancy derivatives of the Lagrange multiplier (averaged inverse screened response functions) are shown, as well as their non-corresponding linear-response approximations (crosses).

connected domains of stability of the unconstrained DFT problem, it cannot deform those domains. This is a consequence of the linearity of E_c in the density and thus its vanishing contribution to the fixed-V_c curvature of W. The constraint may, however cause abrupt transitions of energy minima across disconnected domains, as observed in the "OS(-)" to "OS(+)" transition of Fig. 1 (albeit in the more general case of a spin-dependent constraint).

In order to analyze the sign of the quantity expressed in Eq. 31, we may focus on the DFT energy curvature with respect to the subspace occupancy, $d^2E_{\rm DFT}/dN^2$. Let us suppose that stable ground-states are observed, in a particular constrained system, as V_c is continuously varied within an interval. The local special case of Eq. 26 provides that $dE_{\rm DFT}/d\rho^\sigma(\mathbf{r}) = -v_\sigma^{\rm external}(\mathbf{r}) = -w_c(\mathbf{r})V_c$. Combining this with the general properties of a positive definite matrix, i.e., that its inverse is positive definite and that its diagonal elements are positive, we find that

$$0 < \left(\frac{d^2E_{\rm DFT}}{d\rho^{\sigma 2}}\right)^{-1}(\mathbf{r},\mathbf{r}) = \left(-\frac{dv_\sigma^{\rm external}}{d\rho^\sigma}\right)^{-1}(\mathbf{r},\mathbf{r})$$
$$= -\chi^{\sigma\sigma}(\mathbf{r},\mathbf{r}) = -\frac{d\rho^\sigma(\mathbf{r})}{dv_\sigma^{\rm external}(\mathbf{r})} = -\frac{d\rho^\sigma(\mathbf{r})}{w_c^\sigma(\mathbf{r})\,dV_c}. \quad (33)$$

Following from this, we may multiply by $(w_c^\sigma(\mathbf{r}))^2$, allowing $w_c^\sigma(\mathbf{r})$ to take zero (but not at all $\mathbf{r}$) and negative values, as is necessary, for example, when constraining the difference in charge between two regions. Then, integrating over all space, we arrive at the result

$$0 > \sum_\sigma \int (w_c^\sigma(\mathbf{r}))^2 \frac{d\rho^\sigma(\mathbf{r})}{w_c^\sigma(\mathbf{r})\,dV_c}\,d\mathbf{r} = \frac{dN}{dV_c} = \chi. \quad (34)$$

Thus, Eq. 33, which states that the local part of the interacting response function is negative about stable ground-states, is generalized in Eq. 34 to the cDFT response function for an arbitrary weight function, irrespective of its profile or even its sign. Recalling Eq. 14, we arrive at the sought-after result that $d^2W/dV_c^2 < 0$ over stable ground-states. We note that this result is valid up to arbitrary order in response, it is general to degenerate and non-degenerate systems, and it accounts for screening.

Conversely, let us briefly suppose that $d^2W/dV_c^2 \geq 0$ for some value of V_c. Then, by virtue of Eq. 14, we have $dN/dV_c \geq 0$ and, combining Eq. 33, Eq. 34, and the non-negativity of $(w_c^\sigma(\mathbf{r}))^2$, there exist $\mathbf{r}$ and σ for which $w_c^\sigma(\mathbf{r}) \neq 0$ and $0 \geq \left(d^2E_{\rm DFT}/d\rho^{\sigma 2}\right)^{-1}(\mathbf{r},\mathbf{r})$. Then, $\left(d^2E_{\rm DFT}/d\rho^\sigma d\rho^{\sigma'}\right)^{-1}(\mathbf{r},\mathbf{r}')$ may not be positive definite since it has a non-positive diagonal element. Therefore, its inverse $\left(d^2E_{\rm DFT}/d\rho^\sigma d\rho^{\sigma'}\right)(\mathbf{r},\mathbf{r}')$ may also not be positive definite, and this guarantees that the state is unstable with respect to spin-density perturbations. Then, only meta-stable states such as the "CS" state depicted in Fig. 1 may be observed in practice. There are two ways in which cDFT inflection points may arise, that is, cases where $d^2W/dV_c^2 = dN/dV_c = 0$. First, the constraint may couple pathologically to the density or not couple to it at all. Trivial examples of this are constraints where, for all σ and $\mathbf{r}$, $w_c^\sigma(\mathbf{r}) = 1$ or $w_c^\sigma(\mathbf{r})\,\rho^\sigma(\mathbf{r}) = 0$, which result in a vanishing response χ. Second, the state may be degenerate on a line or higher surface, and the constraint may be contrived so as not to break this degeneracy.

Combining these arguments, we conclude that the stability of ground-states over an interval of V_c both implies and requires that d^2W/dV_c^2 remains negative and finite at constrained ground-states within that interval. In practice, this means that intervals of positive curvature are not numerically observable, because unstable or meta-stable states cannot be sampled in a continuous manner. It is however possible, as demonstrated in Fig. 1, to observe numerical discontinuities in the otherwise concave total-energy W, for fixed N_c, when the response, and hence energy curvature, diverges at a phase transition. Such transitions occur at vanishing values of the quantity expressed in Eq. 31, i.e., at inflection points of $E_{\rm DFT}(N)$. For this, it is necessary for $\chi^{\sigma\sigma}(\mathbf{r},\mathbf{r})$ to diverge for some σ and $\mathbf{r}$ where $w_c^\sigma(\mathbf{r}) \neq 0$, by virtue of Eqs. 28, 33 and 34.

VI. MULTIPLE CONSTRAINTS, THE CDFT CONDITION NUMBER, AND THE EXTENSION TO SELF-CONSISTENT FIELD CDFT

In this section, we consider, in detail, the extent to which our principal results may be generalized to multiple constraints, and thereafter to self-consistent field cDFT. For the former, it is helpful to consider a vector Lagrange multiplier $\mathbf{V}_c$, acting upon a vector of constraint functionals $\mathbf{C} = \mathbf{N} - \mathbf{N}_c$, yielding $E_c = \mathbf{V}_c \cdot \mathbf{C}$.

The multivariate generalization of Eq. 28 is the equation

$$\left(\frac{d^2W}{d\mathbf{V}_c^2}\right)^{-1} = \left(\frac{d\mathbf{N}}{d\mathbf{V}_c}\right)^{-1} = \boldsymbol{\chi}^{-1} = \frac{d\mathbf{V}_c}{d\mathbf{N}} = -\frac{d^2E_{\mathrm{DFT}}}{d\mathbf{N}^2}, \tag{35}$$

where the negative exponent denotes matrix inversion, and the matrix is symmetric due to the symmetry of $\chi(\mathbf{r},\mathbf{r}')$ under co-ordinate exchange in Eq. 13. We may also consider the non-interacting analogue of Eq. 35, viz.

$$\left(\frac{d^2W}{d\mathbf{V}d\mathbf{V}_c}\right)^{-1} = \left(\frac{d\mathbf{N}}{d\mathbf{V}}\right)^{-1} = \boldsymbol{\chi}_0^{-1}. \tag{36}$$

Similar expressions may be derived for the second derivatives of E_{DFT} and E_c. For example, Eq. 21 becomes, noting that the final object is a rank-three tensor,

$$\frac{d^2E_{\mathrm{DFT}}}{d\mathbf{V}d\mathbf{V}_c} = -\boldsymbol{\chi}_0 - \mathbf{V}_c\cdot\frac{d\boldsymbol{\chi}_0}{d\mathbf{V}_c}. \tag{37}$$

The dielectric function may also be straightforwardly generalised in order to describe the coupling of dielectric screening between constrained subspaces. In the spin-degenerate or spin-averaged case, it takes the particularly simple matrix form

$$\boldsymbol{\epsilon} = \frac{d\mathbf{V}_c}{d\mathbf{V}} = \frac{1}{2}\boldsymbol{\chi}_0\cdot\boldsymbol{\chi}^{-1}. \tag{38}$$

The behaviour of multivariate cDFT optimisation depends on the nature of the energy landscape with respect to $\mathbf{V}_c$, and it may be complicated by the presence of multiple extrema or by surfaces which are elongatated in some directions relatively to others. The curvature of the energy landscape, about a particular value of $\mathbf{V}_c$, is characterized by the eigenvalues of the Hessian matrix $\boldsymbol{\chi}$. These must be identical for optimal extremization of $W[\mathbf{V}_c]$ by simple conjugate gradients. More generally, the positive-valued condition number k, defined by

$$k^2 = \sum_{IJ}\left(\left[\frac{d^2W}{d\mathbf{V}_c^2}\right]_{IJ}\right)^2\sum_{KL}\left(\left[\frac{d^2W}{d\mathbf{V}_c^2}\right]^{-1}_{KL}\right)^2, \tag{39}$$

where capitalized letters index constraints, gives a measure of the spread of the Hessian eigenvalues. The optimization problem is said to be ill-conditioned if k is much larger than one. Then, conjugate gradients may be expected to perform poorly, and Newton or quasi-Newton methods may be considered. We may rephrase k as

$$\begin{aligned} k^2 &= \sum_{IJ}\left(\left[\frac{d\mathbf{N}}{d\mathbf{V}_c}\right]_{IJ}\right)^2\sum_{KL}\left(\left[\frac{d\mathbf{V}_c}{d\mathbf{N}}\right]_{KL}\right)^2 \\ &= \sum_{IJ}\left([\boldsymbol{\chi}]_{IJ}\right)^2\sum_{KL}\left(\left[\boldsymbol{\chi}^{-1}\right]_{KL}\right)^2 \\ &= \sum_{IJ}\left(\left[\left(\frac{d^2E_{\mathrm{DFT}}}{d\mathbf{N}^2}\right)^{-1}\right]_{IJ}\right)^2\sum_{KL}\left(\left[\frac{d^2E_{\mathrm{DFT}}}{d\mathbf{N}^2}\right]_{KL}\right)^2, \end{aligned} \tag{40}$$

through which it is clear that $W[\mathbf{V}_c]$ has the same condition number as $E_{\mathrm{DFT}}[\mathbf{N}_c]$. If optimising $\mathbf{V}_c$ during the density update step of self-consistent field DFT codes[4,56], the corresponding condition number k_0 may be calculated using the fixed-potential equivalent of Eq. 40. Both k and k_0 are amenable to evaluation by finite differences. If the response $\boldsymbol{\chi}$ or inverse response $\boldsymbol{\chi}^{-1}$ matrices are singular, k diverges, the problem is said to be ill-posed, and its definition must be reconsidered. We refer the reader to Ref. 73 for a more general discussion of condition numbers in the context of electronic structure.

The connection between the stability of constrained states and the negativity of d^2W/dV_c^2, as demonstrated in Section V, is here generalized to the multivariate case. More precisely, the stability of multiply-constrained ground-states both implies and requires that the matrix $d^2W/d\mathbf{V}_c^2$ has strictly negative diagonal elements. If the matrix is strictly diagonally dominant, furthermore, stability implies and requires that $W(\mathbf{V}_c)$ is strictly concave locally. To see this, let us assume that stable ground-states are observed as $\mathbf{V}_c$ is varied within some simply connected volume. Then, taking the diagonal matrix elements of $d^2W/d\mathbf{V}_c^2$ individually, while following Eqs. 33 and 34 for each constraint labelled I, we find that

$$0 > \sum_\sigma\int\left(w_{cI}^\sigma(\mathbf{r})\right)^2\frac{d\rho^\sigma(\mathbf{r})}{w_{cI}^\sigma(\mathbf{r})\,dV_{cI}}\,d\mathbf{r} = \left[\frac{d\mathbf{N}}{d\mathbf{V}_c}\right]_{II}. \tag{41}$$

Combining this with Eq. 35, we deduce that the diagonal matrix elements of $d^2W/d\mathbf{V}_c^2$ are all negative. This is a necessary but not sufficient condition for $d^2W/d\mathbf{V}_c^2$ to be negative definite locally. However, it becomes a sufficient condition for negative definiteness if the symmetric matrix is also diagonally dominant[?] . Diagonal dominance is a physically reasonable, albeit system-dependent, condition related to the extent of non-locality in $\chi(\mathbf{r},\mathbf{r}')$. If it holds, stability implies that $W(\mathbf{V}_c)$ is strictly concave locally. Additionally, if $w_{cJ}^\sigma(\mathbf{r})\,w_{cI}^\sigma(\mathbf{r}) > 0$ for all I, J, σ, and $\mathbf{r}$ (such as if $w_{cI}^\sigma(\mathbf{r}) > 0$ for all I and σ), then

$$0 > \sum_\sigma\int w_{cJ}^\sigma(\mathbf{r})\,w_{cI}^\sigma(\mathbf{r})\frac{d\rho^\sigma(\mathbf{r})}{w_{cI}^\sigma(\mathbf{r})\,dV_{cI}}\,d\mathbf{r}, \tag{42}$$

and the Hessian is a strictly negative matrix, but that alone does not imply its negative definiteness. Conversely, if $d^2W/d\mathbf{V}_c^2$ does not exhibit all negative diagonal elements, as is possible if it is not negative definite, for example, then, $[d\mathbf{N}/d\mathbf{V}_c]_{II} \geq 0$ for one or more values of I. Then, by the non-negativity of $\left(w_{cI}^\sigma(\mathbf{r})\right)^2$ for all I, σ, and $\mathbf{r}$, the state is unstable, as previously shown in the single-constraint case. Thus, we conclude that if a ground-state subject to multiple linear, non-trivial constraints is stable with respect to perturbations, and hence locatable by numerical cDFT optimization, this implies and requires that the associated Hessian matrix $d^2W/d\mathbf{V}_c$ has a strictly negative diagonal, and that it is negative definite in the event that it is diagonally dominant. If it is not strictly diagonally dominant, however,

we cannot rule out the possibility of stable ground-states occurring at saddle points of the self-consistent $W(\mathbf{V}_c)$.

Finally, we consider the energy landscape associated with cDFT Lagrange multiplier optimization within the fixed-potential inner loop of self-consistent field DFT codes. For this, let us first assume that stable minimum energy eigenstates are observed, for a given fixed DFT contribution $\hat{v}_\sigma^{\mathrm{DFT}}$ to the Kohn-Sham potential, as $\mathbf{V}_c$ is varied within some simply connected volume. Again, we may analyze the diagonal matrix elements of $d^2W/d\mathbf{V}_c^2$ individually, but in this case $dv_\sigma^{\mathrm{KS}}(\mathbf{r}) = dv_\sigma^{\mathrm{external}}(\mathbf{r}) = w_{cI}^\sigma(\mathbf{r})\, dV_{cI}^\sigma$, for each I, and for all σ and $\mathbf{r}$. Then, Eq. 33 may be modified for a fixed DFT potential, to give

$$0 < \left(\frac{d^2E_{\mathrm{DFT}}}{d\rho^{\sigma 2}}\right)^{-1}_{\hat{v}_\sigma^{\mathrm{DFT}}}(\mathbf{r},\mathbf{r}) = -\left.\frac{d\rho^\sigma(\mathbf{r})}{w_{cI}^\sigma(\mathbf{r})\, dV_{cI}}\right|_{\hat{v}_\sigma^{\mathrm{DFT}}}, \quad (43)$$

whereupon Eq. 41 may be similarly adapted, yielding

$$0 > \sum_\sigma \int \left.\frac{w_{cI}^\sigma(\mathbf{r})\, d\rho^\sigma(\mathbf{r})}{dV_{cI}}\right|_{\hat{v}_\sigma^{\mathrm{DFT}}} d\mathbf{r} = \left[\frac{d\mathbf{N}}{d\mathbf{V}_c}\right]^{\hat{v}_\sigma^{\mathrm{DFT}}}_{II}. \quad (44)$$

The identity $d^2\mathbf{W}/dV_c^2 = d\mathbf{N}/d\mathbf{V}_c$ remains valid for a fixed $\hat{v}_\sigma^{\mathrm{DFT}}$, since it relies only on the orthonormality of Kohn-Sham eigenstates. Thus, the diagonal elements of $d^2\mathbf{W}/dV_c^2$ are individually negative, and the guarantee of strict local concavity of $W(\mathbf{V}_c)$, for any given $\hat{v}_\sigma^{\mathrm{DFT}}$, is again conditional on a symmetric diagonally dominant? $d^2\mathbf{W}/dV_c^2$. If the matrix does not exhibit a strictly negative diagonal, conversely, then $[d\mathbf{N}/d\mathbf{V}_c]_{II} \geq 0$ for one or more values of I, and there exist $\mathbf{r}$ and σ for which $w_c^\sigma(\mathbf{r}) \neq 0$ and $0 \geq \left(d^2E_{\mathrm{DFT}}/d\rho^{\sigma 2}\right)^{-1}(\mathbf{r},\mathbf{r})$ at fixed $\hat{v}_\sigma^{\mathrm{DFT}}$. Then, the non-self-consistent $\left(d^2E_{\mathrm{DFT}}/d\rho^\sigma d\rho^{\sigma'}\right)(\mathbf{r},\mathbf{r}')$ cannot be positive definite, and the state is unstable. We conclude that for a minimum-energy eigenstate, given a fixed DFT potential and subject to one or more linear, non-trivial constraints, to be stable with respect to perturbations and hence locatable by SCF-type cDFT optimization, it implies and requires the associated fixed-$\hat{v}_\sigma^{\mathrm{DFT}}$ Hessian matrix $d^2W/d\mathbf{V}_c$ to have a strictly negative diagonal, and for it to be negative definite in the event that it is diagonally dominant. This generalizes the results of Refs. 1, 4, and 5 beyond the first-order non-degenerate perturbative regime, extending their validity to systems which exhibit non-linear response or orbital degeneracy.

VII. CONCLUSION AND SUMMARY

Constrained DFT is an flexible, potent approach that broadens the scope and flexibility of DFT-based atomistic simulation. A growing number of software implementations of cDFT are now appearing[1,24,26,29,30,52,74–79], including linear-scaling implementations designed for application to large systems[18,53]. It is inherently parallelizable, and thus potentially suitable for use in combination with high-throughput materials screening infrastructures[50,51]. Fundamental developments will be required to bring cDFT into the realm of such very routine use. For transferability and comparability between codes, for example, the standardized, automated selection of population analysis and targeting schemes, ideally but not necessarily based on energy considerations, would surely be beneficial. Methods based on promolecule densities[46] or self-consistent Wannier functions[80] are promising possibilities in this direction. The key findings and conclusions of the present work are that:

- For any self-consistent energy second-derivative with respect to a constrained expectation value, there is an equivalent integrated linear response or inverse-response function which is more convenient to calculate. This provides a basis for future quasi-Newton or preconditioning approaches for cDFT.
- A negative-diagonal self-consistent cDFT Hessian is implied by the local stability of the system with respect to perturbations about the point of evaluation. A Hessian lacking this property cannot be observed by finite differences, and so may be excluded in automation. This generalizes W&VV's result to the self-consistent cDFT problem, the non-linear response regime, and to degenerate orbitals.
- Concave regions in the DFT energy versus spin-density landscape cannot be explored using cDFT.
- Integrated response and dielectric functions may be evaluated as by-products of cDFT optimization, without sums over empty Kohn-Sham eigenstates.
- Existing cDFT optimization schemes based on the self-consistent field approach, which update the cDFT Lagrange multipliers with fixed DFT potentials, may be readily adapted for the self-consistent gradients required in direct-minimization DFT.
- cDFT does not change the domains of stability of the underlying DFT energy landscape, it moves the solutions around, or between, these domains. When there are two or more such domains in cDFT, it is possible to observe multiple solutions, hysteresis, and energy discontinuities at such transitions.

We expect that this work may facilitate the advanced automation of cDFT Lagrange multiplier optimization, particularly in the high-throughput, molecular dynamics, and linear-scaling regimes. Our general framework for treating energy landscapes in terms of integrated response functions now enables the extension of cDFT to new areas of atomistic and continuum simulation.

ACKNOWLEDGEMENTS

This work was enabled by the Royal Irish Academy – Royal Society International Exchange Cost Share Pro-

gramme (IE131505). GT acknowledges support from EPSRC UK (EP/I004483/1 and EP/K013610/1). We acknowledge and thank the ONETEP Developer's Group for hosting workshops that facilitated this development, and Qin Wu for a helpful communication and discussion.

Appendix A: Approximate connection of the cDFT non-interacting response function to unscreened sum-over-states perturbation theory

In this Appendix, we investigate how the non-interacting linear-response function defined by $\chi_0 = dN/dV = d^2W/dVdV_c$ in Eq. 19 relates to the unscreened sum-over-states perturbation theory expression given by Eq. 7 of Ref. 5. The latter is obtained by replacing $\left(\varepsilon^{-1}w_c\right)^\sigma$ by w_c^σ in Eq. 11. It yields the linear response of the targeted density N to a change in the subspace-averaged Kohn-Sham potential V with all other aspects of the Kohn-Sham potential kept fixed. Its evaluation for two values of V_c, close to those at which E_c and W assume maxima, is shown in Fig. 5 (solid circles). The proximity of these data points to $d^2E_c/dVdV_c$ is perhaps not entirely coincidental, but they sit rather far from their most closely related quantity, dN/dV. The difference between the sum-over-states expression and dN/dV is subtle, since both are non-interacting response functions with the same integration. It arises due to complex spatial fluctuations in $v_\sigma^{\mathrm{KS}}(\mathbf{r})$ both within and without the weighted region in the case of dN/dV, in contrast to the effective $\delta v_\sigma^{\mathrm{KS}}(\mathbf{r}) = w_c^\sigma(\mathbf{r})\,\delta V$ implied in the sum-over-states expression. More precisely, dN/dV is the complete non-interacting linear-response function, whereas the sum-over-states is the non-interacting linear-response function truncated at first-order in perturbation theory.

Referring to Eq. 11, the dN/dV calculated using self-consistent cDFT simplifies to the perturbation theory expression in the case that both $dv_\sigma^{\mathrm{KS}}(\mathbf{r})/dV^\sigma = w_c^\sigma(\mathbf{r})$ and the change in the average weighted Kohn-Sham potential V^σ is the wholly responsible for the change in subspace occupancy N, with all other degrees of freedom fixed. The first condition and Eq. 17 together imply that

$$\begin{aligned} 1 &\equiv \int \left(\frac{dV^\sigma}{dv_\sigma^{\mathrm{KS}}(\mathbf{r})}\right)\left(\frac{dv_\sigma^{\mathrm{KS}}(\mathbf{r})}{dV^\sigma}\right) d\mathbf{r} \\ &= \left(\int w_c^\sigma(\mathbf{r}')\; d\mathbf{r}'\right)^{-1} \int \left(w_c^\sigma(\mathbf{r})\right)^2\; d\mathbf{r}, \end{aligned} \tag{A1}$$

which would be readily satisfied only if $w_c^\sigma(\mathbf{r})$ were an abrupt three dimensional unit step function.

The second condition is more unrealistic, since we may directly vary the Lagrange multiplier V_c when constraining DFT, but not, at least directly, the average subspace Kohn-Sham potential V^σ. As V_c is varied, self-consistent changes in $v_\sigma^{\mathrm{KS}}(\mathbf{r})$ outside of the weighted region may substantially mitigate the charge transfer due to changes within it. Such effects are absent at first order in perturbation theory, and so it may be expected to typically overestimate the magnitude of the non-interacting response dN/dV, a situation which is exemplified in Fig. 5.

Since the differences in definition between the non-interacting linear and sum-over-states response functions are related, albeit not entirely, to effects outside of the weighted region, they cannot be reconciled. An approximate reconciling renormalization may be made, however, by down-scaling one of the two functions $w_c^\sigma(\mathbf{r})$ in the unscreened analogue of Eq. 11 (one applies the perturbation, the other measures the charge) by a factor of $\sum_\sigma \left(\int w_c^\sigma(\mathbf{r})\; d\mathbf{r}\right) / \left(\int\; d\mathbf{r}'\right)$. This scaling mimics the compensating background changes in the Kohn-Sham potential in the realistic cDFT calculation, by reducing or "redistributing" the change in potential $w_c^\sigma(\mathbf{r})\,\delta V^\sigma$ in proportion to the system volume. The result of this renormalization, suitably adapted for orbital-based population analysis (based on orbital count, with the advantage that the rescaling is not extensive with respect to the volume of the vacuum region), is shown in open black circles in Fig. 5. We find that the unscreened sum-over-states expression is thus brought into fair, but not exact, agreement with the non-perturbative non-interacting response dN/dV. A further downscaling by a factor of the integrated inverse microscopic dielectric function, given by Eq. 22, is then required to approximately match the unscreened sum-over-states perturbation theory and self-consistent cDFT total-energy curvatures.

* daithi.o.riogain@tcd.ie
† g.teobaldi@liverpool.ac.uk

[1] B. Kaduk, T. Kowalczyk, and T. Van Voorhis, Chemical Reviews **112**, 321 (2012).
[2] P. Hohenberg and W. Kohn, Phys. Rev. **136**, B864 (1964).
[3] W. Kohn and L. J. Sham, Phys. Rev. **140**, A1133 (1965).
[4] Q. Wu and T. Van Voorhis, Journal of Chemical Theory and Computation **2**, 765 (2006).
[5] Q. Wu and T. Van Voorhis, Phys. Rev. A **72**, 024502 (2005).
[6] M. Segal, M. Singh, K. Rivoire, S. Difley, T. Van Voorhis, and M. A. Baldo, Nature Materials **6**, 374 (2007).
[7] T. Kowalczyk, Z. Lin, and T. V. Voorhis, The Journal of Physical Chemistry A **114**, 10427 (2010).

[8] P. H. Dederichs, S. Blügel, R. Zeller, and H. Akai, Phys. Rev. Lett. **53**, 2512 (1984).
[9] Q. Wu and T. Van Voorhis, The Journal of Physical Chemistry A **110**, 9212 (2006).
[10] H. Oberhofer and J. Blumberger, The Journal of Chemical Physics **131**, 064101 (2009).
[11] P. H.-L. Sit, M. Cococcioni, and N. Marzari, Phys. Rev. Lett. **97**, 028303 (2006).
[12] T. Tim Kowalczyk, L.-P. Wang, and T. Van Voorhis, The Journal of Physical Chemistry B **115**, 12135 (2011).
[13] J. Behler, K. Reuter, and M. Scheffler, Phys. Rev. B **77**, 115421 (2008).
[14] I. Rudra, Q. Wu, and T. Van Voorhis, The Journal of Chemical Physics **124**, 024103 (2006).
[15] I. Rudra, Q. Wu, and T. Van Voorhis, Inorganic Chemistry **46**, 10539 (2007).
[16] J. R. Schmidt, N. Shenvi, and J. C. Tully, The Journal of Chemical Physics **129**, 114110 (2008).
[17] S. Difley, D. Beljonne, and T. Troy Van Voorhis, Journal of the American Chemical Society **130**, 3420 (2008).
[18] A. M. P. Sena, T. Miyazaki, and D. R. Bowler, Journal of Chemical Theory and Computation **7**, 884 (2011).
[19] D. H. P. Turban, G. Teobaldi, D. D. O'Regan, and N. D. M. Hine, Phys. Rev. B **93**, 165102 (2016).
[20] E. Runge and E. K. U. Gross, Phys. Rev. Lett. **52**, 997 (1984).
[21] S. Difley and T. Van Voorhis, Journal of Chemical Theory and Computation **7**, 594 (2011).
[22] K. Nakamura, Y. Yoshimoto, R. Arita, S. Tsuneyuki, and M. Imada, Phys. Rev. B **77**, 195126 (2008).
[23] S. Roychoudhury, C. Motta, and S. Sanvito, Phys. Rev. B **93**, 045130 (2016).
[24] A. M. Souza, I. Rungger, C. D. Pemmaraju, U. Schwingenschloegl, and S. Sanvito, Phys. Rev. B **88**, 165112 (2013).
[25] J. D. Sau, J. B. Neaton, H. J. Choi, S. G. Louie, and M. L. Cohen, Phys. Rev. Lett. **101**, 026804 (2008).
[26] C. Brooke, A. Vezzoli, S. J. Higgins, L. A. Zotti, J. J. Palacios, and R. J. Nichols, Phys. Rev. B **91**, 195438 (2015).
[27] Q. Wu and T. Van Voorhis, The Journal of Chemical Physics **125**, 164105 (2006).
[28] F. Ding, H. Wang, Q. Wu, T. Van Voorhis, S. Chen, and J. P. Konopelski, The Journal of Physical Chemistry A **114**, 6039 (2010).
[29] H. Oberhofer and J. Blumberger, J. Chem. Phys. **131**, 064101 (2009).
[30] H. Oberhofer and J. Blumberger, J. Chem. Phys. **133**, 244105 (2010).
[31] A. Kubas, F. Hoffmann, A. Heck, H. Oberhofer, M. Elstner, and J. Blumberger, J. Chem. Phys. **140**, 104105 (2014).
[32] A. Kubas, F. Gajdos, A. Heck, H. Oberhofer, M. Elstner, and J. Blumberger, Phys. Chem. Chem. Phys. **17**, 14342 (2015).
[33] H. Oberhofer and J. Blumberger, Angew. Chem. Int. Ed. **49**, 3631 (2010).
[34] H. Oberhofer and J. Blumberger, Phys. Chem. Chem. Phys. **14**, 13846 (2012).
[35] K. P. McKenna and J. Blumberger, Phys. Rev. B **86**, 245110 (2012).
[36] J. Blumberger and K. P. McKenna, Phys. Chem. Chem. Phys. **15**, 2184 (2013).
[37] S. Yeganeh and T. Van Voorhis, The Journal of Physical Chemistry C **114**, 20756 (2010).
[38] S. R. Yost, J. Lee, M. W. B. Wilson, T. Wu, D. P. McMahon, R. R. Parkhurst, N. J. Thompson, D. N. Congreve, A. Rao, K. Johnson, M. Y. Sfeir, M. G. Bawendi, T. M. Swager, R. H. Friend, M. A. Baldo, and T. Van Voorhis, Nat. Chem. **6**, 492 (2014).
[39] J. S. Evans, C.-L. Cheng, and T. Van Voorhis, Phys. Rev. B **78**, 165108 (2008).
[40] V. I. Anisimov, J. Zaanen, and O. K. Andersen, Phys. Rev. B **44**, 943 (1991).
[41] H. Meider and M. Springborg, Journal of Physics: Condensed Matter **10**, 6953 (1998).
[42] P. L. Danielsen, Journal of Physics C: Solid State Physics **19**, L741 (1986).
[43] H. Meider and M. Springborg, Chemical Physics Letters **300**, 339 (1999).
[44] M. S. Hybertsen, M. Schlüter, and N. E. Christensen, Phys. Rev. B **39**, 9028 (1989).
[45] A. G. Petukhov, I. I. Mazin, L. Chioncel, and A. I. Lichtenstein, Phys. Rev. B **67**, 153106 (2003).
[46] Q. Wu, C.-L. Cheng, and T. Van Voorhis, The Journal of Chemical Physics **127**, 164119 (2007).
[47] Q. Wu, B. Kaduk, and T. Van Voorhis, The Journal of Chemical Physics **130**, 034109 (2009).
[48] B. Kaduk and T. Van Voorhis, The Journal of Chemical Physics **133**, 061102 (2010).
[49] B. Kaduk, T. Tsuchimochi, and T. Van Voorhis, The Journal of Chemical Physics **140** (2014).
[50] A. Jain, G. Hautier, C. J. Moore, S. P. Ong, C. C. Fischer, T. Mueller, K. A. Persson, and G. Ceder, Computational Materials Science **50**, 2295 (2011).
[51] S. Curtarolo, G. L. W. Hart, M. B. Nardelli, N. Mingo, S. Sanvito, and O. Levy, Nat Mater **12**, 191 (2013).
[52] J. Řezáč, B. Lévy, I. Demachy, and A. de la Lande, Journal of Chemical Theory and Computation **8**, 418 (2012).
[53] L. E. Ratcliff, L. Genovese, S. Mohr, and T. Deutsch, The Journal of Chemical Physics **142**, 234105 (2015).
[54] The "curvature" is used here as a convenient shorthand for the second derivative. We do not imply the geometric curvature, which equals the second derivative only at stationary points.
[55] Q. Wu, personal communication (2016).
[56] Q. Wu and W. Yang, The Journal of Chemical Physics **118**, 2498 (2003).
[57] C.-K. Skylaris, P. D. Haynes, A. A. Mostofi, and M. C. Payne, The Journal of Chemical Physics **122**, 084119 (2005).
[58] J. P. Perdew, K. Burke, and M. Ernzerhof, Phys. Rev. Lett. **77**, 3865 (1996).
[59] C. Coulson and I. Fischer, Philos. Mag. **40**, 386 (1949).
[60] A. Ruzsinszky, J. P. Perdew, and G. I. Csonka, The Journal of Physical Chemistry A **109**, 11006 (2005).
[61] J. Dziedzic, H. H. Helal, C.-K. Skylaris, A. A. Mostofi, and M. C. Payne, EPL (Europhysics Letters) **95**, 43001 (2011).
[62] O. Andreussi, I. Dabo, and N. Marzari, The Journal of Chemical Physics **136**, 064102 (2012).
[63] A single, strictly local occupancy constraint is considered in Ref. 5. We retain these restrictions so as not to obscure the fundamental aspects under consideration. These conditions are typically lifted in practical cDFT calculations, bringing us into multivariate optimisation of constrained Kohn-Sham spin-density functional theory, which may also be non-local or orbital dependent.
[64] S. Baroni, P. Giannozzi, and A. Testa, Phys. Rev. Lett.

58, 1861 (1987).
[65] S. Baroni, S. de Gironcoli, A. Dal Corso, and P. Giannozzi, Rev. Mod. Phys. **73**, 515 (2001).
[66] We use a lunate epsilon ϵ for the microscopic dielectric function in order to distinguish from it from the Kohn-Sham eigenvalues ε.
[67] A. D. Becke, Phys. Rev. A **38**, 3098 (1988).
[68] C. Lee, W. Yang, and R. G. Parr, Phys. Rev. B **37**, 785 (1988).
[69] C.-K. Skylaris, A. A. Mostofi, P. D. Haynes, O. Diéguez, and M. C. Payne, Phys. Rev. B **66**, 035119 (2002).
[70] D. D. O'Regan, M. C. Payne, and A. A. Mostofi, Phys. Rev. B **85**, 193101 (2012).
[71] The resulting constraint acts on the Kohn-Sham density-matrix rather than on the density. Our analytical findings extends to that case with minor notational changes.
[72] L. E. Ratcliff, N. D. M. Hine, and P. D. Haynes, Phys. Rev. B **84**, 165131 (2011).
[73] J. M. Rondinelli, B. Deng, and L. D. Marks, Computational Materials Science **40**, 345 (2007).
[74] M. Valiev, E. Bylaska, N. Govind, K. Kowalski, T. Straatsma, H. V. Dam, D. Wang, J. Nieplocha, E. Apra, T. Windus, and W. de Jong, Computer Physics Communications **181**, 1477 (2010).
[75] Y. Shao, Z. Gan, E. Epifanovsky, A. T. B. Gilbert, M. Wormit, J. Kussmann, A. W. Lange, A. Behn, J. Deng, X. Feng, D. Ghosh, M. Goldey, P. R. Horn, L. D. Jacobson, I. Kaliman, R. Z. Khaliullin, T. Kús, A. Landau, J. Liu, E. I. Proynov, Y. M. Rhee, R. M. Richard, M. A. Rohrdanz, R. P. Steele, E. J. Sundstrom, H. L. Woodcock III, P. M. Zimmerman, D. Zuev, B. Albrecht, E. Alguire, B. Austin, G. J. O. Beran, Y. A. Bernard, E. Berquist, K. Brandhorst, K. B. Bravaya, S. T. Brown, D. Casanova, C.-M. Chang, Y. Chen, S. H. Chien, K. D. Closser, D. L. Crittenden, M. Diedenhofen, R. A. DiStasio Jr., H. Dop, A. D. Dutoi, R. G. Edgar, S. Fatehi, L. Fusti-Molnar, A. Ghysels, A. Golubeva-Zadorozhnaya, J. Gomes, M. W. D. Hanson-Heine, P. H. P. Harbach, A. W. Hauser, E. G. Hohenstein, Z. C. Holden, T.-C. Jagau, H. Ji, B. Kaduk, K. Khistyaev, J. Kim, J. Kim, R. A. King, P. Klunzinger, D. Kosenkov, T. Kowalczyk, C. M. Krauter, K. U. Lao, A. Laurent, K. V. Lawler, S. V. Levchenko, C. Y. Lin, F. Liu, E. Livshits, R. C. Lochan, A. Luenser, P. Manohar, S. F. Manzer, S.-P. Mao, N. Mardirossian, A. V. Marenich, S. A. Maurer, N. J. Mayhall, C. M. Oana, R. Olivares-Amaya, D. P. O'Neill, J. A. Parkhill, T. M. Perrine, R. Peverati, P. A. Pieniazek, A. Prociuk, D. R. Rehn, E. Rosta, N. J. Russ, N. Sergueev, S. M. Sharada, S. Sharmaa, D. W. Small, A. Sodt, T. Stein, D. Stück, Y.-C. Su, A. J. W. Thom, T. Tsuchimochi, L. Vogt, O. Vydrov, T. Wang, M. A. Watson, J. Wenzel, A. White, C. F. Williams, V. Vanovschi, S. Yeganeh, S. R. Yost, Z.-Q. You, I. Y. Zhang, X. Zhang, Y. Zhou, B. R. Brooks, G. K. L. Chan, D. M. Chipman, C. J. Cramer, W. A. Goddard III, M. S. Gordon, W. J. Hehre, A. Klamt, H. F. Schaefer III, M. W. Schmidt, C. D. Sherrill, D. G. Truhlar, A. Warshel, X. Xua, A. Aspuru-Guzik, R. Baer, A. T. Bell, N. A. Besley, J.-D. Chai, A. Dreuw, B. D. Dunietz, T. R. Furlani, S. R. Gwaltney, C.-P. Hsu, Y. Jung, J. Kong, D. S. Lambrecht, W. Liang, C. Ochsenfeld, V. A. Rassolov, L. V. Slipchenko, J. E. Subotnik, T. Van Voorhis, J. M. Herbert, A. I. Krylov, P. M. W. Gill, and M. Head-Gordon, Mol. Phys. **113**, 184 (2015).
[76] P. Kurz, F. Förster, L. Nordström, G. Bihlmayer, and S. Blügel, Phys. Rev. B **69**, 024415 (2004).
[77] T. Ozaki and H. Kino, Phys. Rev. B **72**, 045121 (2005).
[78] J. Hutter, M. Iannuzzi, F. Schiffmann, and J. VandeVondele, Wiley Interdisciplinary Reviews: Computational Molecular Science **4**, 15 (2014).
[79] P.-W. Ma and S. L. Dudarev, Phys. Rev. B **91**, 054420 (2015).
[80] D. D. O'Regan, N. D. M. Hine, M. C. Payne, and A. A. Mostofi, Phys. Rev. B **82**, 081102 (2010).